

On the evolution of rotating accreting white dwarfs and type Ia supernovae

B. Wang,^{1,2*} S. Justham,³ Z.-W. Liu,⁴ J.-J. Zhang,^{1,2} D.-D. Liu^{1,2} and Z. Han^{1,2}

¹*Yunnan Observatories, Chinese Academy of Sciences, Kunming 650011, China*

²*Key Laboratory for the Structure and Evolution of Celestial Objects, Chinese Academy of Sciences, Kunming 650011, China*

³*National Astronomical Observatories, Chinese Academy of Sciences, Beijing 100012, China*

⁴*Argelander-Institut für Astronomie, Auf dem Hügel 71, D-53121, Bonn, Germany*

Accepted 2014 September 9

ABSTRACT

The potential importance of the angular momentum which is gained by accreting white dwarfs (WDs) has been increasingly recognized in the context of type Ia supernova (SN Ia) single-degenerate model. The expectation that the spin of the WD can delay the explosion should help the single-degenerate model to be consistent with the observed properties of most SNe Ia, in particular by avoiding hydrogen contamination. In this article, we attempt to study the most prominent single-degenerate supersoft (WD + MS) channel when the rotation of accreting WDs is considered. We present a detailed binary population synthesis study to examine the predicted population of SNe Ia for this channel. For our standard model, we find that 77% of these SNe Ia explode with WD masses which are low enough to be supported by solid-body rotation ($\leq 1.5 M_{\odot}$); this is a substantially higher proportion than found by previous work. Only 2% have WD explosion masses $\geq 2.0 M_{\odot}$; these require the initial WD mass to be larger than $1.0 M_{\odot}$. We further discuss the possible origin of the diversity of SNe Ia from the pre- and post-accretion properties of the WDs in this population. We also suggest that some SN Ia progenitors with substantial circumstellar hydrogen, including some apparent type II_n SNe, might be related to WDs which required support from differential rotation to avoid explosion, since these can still be accreting from hydrogen-rich donors with a relatively high mass-transfer rate at the time of the SN explosion.

Key words: binaries: close – stars: evolution – supernovae: general – white dwarfs

1 INTRODUCTION

Type Ia supernova (SN Ia) explosions are amongst the most energetic events observed in the Universe, and they are valuable probes for the study of cosmic evolution. Empirical correlations which allow the inference of absolute luminosities from observed lightcurves have enabled SNe Ia to be used as distance indicators. These methods, combined with their visibility to cosmological scales, enabled the determination of the accelerating expansion of the Universe (e.g. Riess et al. 1998; Perlmutter et al. 1999). Even though SNe Ia have been successfully used as standardizable candles for measuring cosmological distances, there exists diversity amongst SNe Ia that is presently not well understood. Nor do we know how

* E-mail: wangbo@ynao.ac.cn

this diversity is linked to the properties of their progenitors and the explosion mechanism. Understanding the variety which is contained within the population of SNe Ia should help to constrain their origin and possible explosion mechanisms. In principle, there might be random reasons why SNe Ia appear different from each other (e.g. the number of ignition points, the location of the deflagration-to-detonation transition or symmetry-breaking produced by aspherical explosions; see, e.g. Hillebrandt & Niemeyer 2000; Röpke & Hillebrandt 2004; Kasen, Röpke & Woosley 2009; Maeda et al. 2010; Chen, Han & Meng 2014). However, the existence of clear systematic population differences suggests that a significant amount of the diversity must arise from systematic causes (for recent observational evidence, see, e.g. Wang & Wheeler 2008; Howell et al. 2009; Sullivan et al. 2010; Childress et al. 2013; Wang et al. 2012, 2013; Pan et al. 2014). These systematic differences seem likely to be able to be traced to the properties of the progenitors, either because of a changing mix of qualitatively different progenitor types or from continuous variation within one progenitor type or both.

It has been widely accepted that SN Ia explosion occurs when a carbon–oxygen white dwarf (CO WD) is destroyed in a thermonuclear explosion. Over the past few decades, two families of models have been proposed to produce CO WDs which reach the conditions necessary for an explosion, i.e. the single-degenerate (SD) and double-degenerate (DD) models. Numerous variants of both the SD and DD scenarios exist (for SD models see, e.g. Whelan & Iben 1973; Hachisu et al. 1996; Li & van den Heuvel 1997; Yungelson & Livio 1998; Langer et al. 2000; Han & Podsiadlowski 2004; Meng, Chen & Han 2009; Wang et al. 2009a; Lü et al. (2009); Ablimit, Xu & Li 2014; Claeys et al. 2014; whilst for DD models see, e.g. Webbink 1984; Iben & Tutukov 1984; Nelemans et al. 2001; van Kerkwijk, Chang & Justham 2010; Chen et al. 2012; Toonen, Nelemans & Portegies Zwart 2012). Different pieces of evidence can be used to support or cause problems for the SD and DD classes, but no definitive arguments have excluded either option. For recent reviews on this subject see Podsiadlowski et al. (2008), Howell (2011), Wang & Han (2012), Parrent, Friesen & Parthasarathy (2014) and Maoz, Mannucci & Nelemans (2014).

In the classic SD model, the WD gains matter from a non-degenerate companion star until it reaches a critical mass limit – near to but not coincident with the Chandrasekhar mass, M_{Ch} – at which the core properties of the WD are expected to result in runaway explosive carbon burning (for a calculation of the critical mass see Nomoto et al. 1997).¹ If the mass-donating companion is a main sequence (MS) star or a slightly evolved star, the formation channel is generally referred to as the “WD + MS channel” even if the mass-donating star is a subgiant star; an alternative name for this is the “supersoft channel” (e.g. Li & van den Heuvel 1997; Langer et al. 2000; Han & Podsiadlowski 2004). This supersoft channel is the most commonly-considered variant of the SD model, and the one which we will concentrate on in this binary population synthesis (BPS) calculations. Additionally, the importance of the rotation of the accreting WD has been increasingly recognized in the context of the SD model (e.g. Yoon & Langer 2004; Justham 2011; Di Stefano, Voss & Claeys 2011; Hachisu et al. 2012a,b). Hachisu et al. (2012a) provided a clear summary of how considering the spin of the WD may be vital to help the SD model be consistent with observations of SNe Ia.

In recent years, a few over-luminous SNe Ia have been observed with inferred WD explosion masses of order $2 M_{\odot}$. SN 2003fg is the first observed over-luminous event. It was discovered on 24 April 2003, and observed to be 2.2 times more luminous than a normal one, and the amount of ^{56}Ni was inferred to be $1.29 \pm 0.07 M_{\odot}$, which would suggest a

¹ For the SD model, however, a vigorous debate is still going on about the process of the mass accretion (see Cassisi, Iben & Tornambè 1998; Idan, Shaviv & Shaviv 2012; Newsham, Starrfield & Timmes 2013).

super-Chandrasekhar mass WD explosion with $M_{\text{WD}} \sim 2.1 M_{\odot}$ (Howell et al. 2006). Following the discovery of SN 2003fg, three over-luminous events were discovered, i.e. SN 2006gz ($M_{\text{Ni}} \sim 1.2 M_{\odot}$; Hicken et al. 2007), SN 2007if ($M_{\text{WD}} \sim 2.4 \pm 0.2 M_{\odot}$ with $M_{\text{Ni}} \sim 1.6 \pm 0.1 M_{\odot}$; Scalzo et al. 2010) and SN 2009dc ($M_{\text{WD}} > 2.0 M_{\odot}$ with $M_{\text{Ni}} = 1.4 - 1.7 M_{\odot}$; Silverman et al. 2011). One possibility is that super-Chandrasekhar mass WDs produce these over-luminous SNe Ia following the mergers of double WD systems (e.g. Howell et al. 2006). If the SD model is to explain the existence of these events, then in these cases the WDs must have been temporarily prevented from exploding by the effect of differential rotation. For the study of the production of these events by SD systems see, e.g. Chen & Li (2009) and Hachisu et al. (2012a,b). Note that models for the luminosity of these events which do not require super-Chandrasekhar mass WDs have been suggested by Hillebrandt, Sim & Röpke (2007) and Hachinger et al. (2012).

Models for SD SN Ia progenitors which include the rotation of WDs find that the SNe should occur from WDs with a range of final mass. The main theoretical uncertainty is whether the accreting WDs are typically able to sustain differential rotation. If differential rotation is easily maintained, then in principle the WD mass distribution at explosion could extend far above M_{Ch} ; for extreme differential rotation, Ostriker & Bodenheimer (1968) calculated that a WD could be stable to be $\sim 4 M_{\odot}$. However, for more realistic conditions, Yoon & Langer (2004) found that some WDs could reach $\sim 2 M_{\odot}$; their adopted angular momentum transport theory required mass-transfer rates in excess of $\sim 3.0 \times 10^{-7} M_{\odot} \text{ yr}^{-1}$ to maintain differential rotation. Hachisu (1986) also suggested the existence of stable equilibrium configurations with $M_{\text{WD}} \geq 2 M_{\odot}$. In contrast, Saio & Nomoto (2004) and Piro (2008) argued that angular-momentum transport is likely to be so efficient that the accreting WD will be forced to approach solid-body rotation. For pure solid-body rotation, the WD stability limit is $\sim 1.47 M_{\odot}$ (Anand 1965; Uenishi, Nomoto & Hachisu 2003; Saio & Nomoto 2004). In this case, the possible mass range of WDs produced by the SD SN Ia models would be restricted to within $\sim 0.1 M_{\odot}$ of the standard ignition mass.

The purpose of this article is to investigate the WD + MS channel systematically when the effect of rotation on the accreting WDs is considered. Firstly, we followed the evolution of the WD + MS binary until the WD increases its mass to the maximum, and thereby obtained the initial and final parameter spaces for the production of SNe Ia. We then used these results to perform a detailed BPS approach in order to obtain SN Ia birthrates and delay times, and the final fate of these systems. This paper is organized as follows. In Section 2, we describe the numerical code for our binary evolution calculations. The binary evolutionary results are shown in Section 3. We describe the BPS method in Section 4 and present the BPS results in Section 5. Finally, a discussion is given in Section 6, and a summary in Section 7.

2 NUMERICAL CODE FOR BINARY EVOLUTION CALCULATIONS

In the WD + MS channel, the Roche-lobe filling star is a MS star or a slightly evolved subgiant star. The mass-donating star transfers some of its matter to the surface of the WD, which leads to the mass increase of the WD. In the previous works (e.g. Han & Podsiadlowski 2004; Meng, Chen & Han 2009; Wang, Li & Han 2010), we stopped the evolution of the WD + MS binary at the moment when the WD increases its mass to $1.378 M_{\odot}$ (i.e. the critical mass limit of non-rotating WDs for carbon ignition; Nomoto et al. 1984). In the present works, however, we further follow the evolution of the WD + MS binary until the mass-transfer rate, $|\dot{M}_2|$, decreases to a critical rate, $3.0 \times 10^{-7} M_{\odot} \text{ yr}^{-1}$ ($= \dot{M}_r$), since the WD is expected to be supported by a strong differential rotation until then (e.g. Yoon & Langer 2004). We assume that the WD can no longer increase in mass when $|\dot{M}_2| < \dot{M}_r$.

for the differential rotation population (see also Chen & Li 2009; Hachisu et al. 2012a,b). Note that this assumption is only applied to the differential rotation population (no critical accretion rate is in principle needed to sustain solid-body rotation).

By using the Eggleton stellar evolution code (Eggleton 1973), we have calculated the evolution of the WD + MS systems. The input physics for this code was updated over the past four decades (Han, Podsiadlowski & Eggleton 1994; Pols et al. 1995, 1998; Nelson & Eggleton 2001; Eggleton & Kiseleva-Eggleton 2002). The description of Roche-lobe overflow from Han, Tout & Eggleton (2000) is adopted. The ratio of mixing length to local pressure scale height is set to be 2.0, and the convective overshooting parameter, δ_{OV} , to be 0.12, which roughly corresponds to an overshooting length of ~ 0.25 pressure scale heights (e.g. Pols et al. 1997). A typical Population I composition is used, i.e. metallicity $Z = 0.02$, H abundance $X = 0.70$ and He abundance $Y = 0.28$.

The prescription of Hachisu et al. (1999) is adopted for the mass growth of the WD by accretion of H-rich matter from its mass-donating star (for details see Han & Podsiadlowski 2004; Wang, Li & Han 2010). If the mass-transfer rate $|\dot{M}_2|$ is above a critical rate, \dot{M}_{cr} , we assume that the accreted H steadily burns on the surface of the WD with a rate of \dot{M}_{cr} , and that the unprocessed matter is lost from the system as an optically thick wind at a mass-loss rate $\dot{M}_{\text{wind}} = |\dot{M}_2| - \dot{M}_{\text{cr}}$ (Hachisu, Kato & Nomoto 1996). The critical mass-transfer rate is

$$\dot{M}_{\text{cr}} = 5.3 \times 10^{-7} \frac{(1.7 - X)}{X} (M_{\text{WD}}/M_{\odot} - 0.4) M_{\odot} \text{yr}^{-1}, \quad (1)$$

in which X is the H mass fraction and M_{WD} is the mass of the WD.

We adopt the following assumptions when $|\dot{M}_2|$ is smaller than \dot{M}_{cr} . (1) When $|\dot{M}_2|$ is less than \dot{M}_{cr} but higher than $\dot{M}_{\text{st}} = \frac{1}{2}\dot{M}_{\text{cr}}$, the H-shell burning is steady and no mass is lost from the system. (2) When $|\dot{M}_2|$ is lower than \dot{M}_{st} but higher than $\dot{M}_{\text{low}} = \frac{1}{8}\dot{M}_{\text{cr}}$, a very weak H-shell flash is triggered but no mass is lost from the system. (3) When $|\dot{M}_2|$ is lower than \dot{M}_{low} , the H-shell flash is so strong that no material is accumulated onto the surface of the WD. We define the mass-growth rate of the He layer under the H-shell burning as

$$\dot{M}_{\text{He}} = \eta_{\text{H}} |\dot{M}_2|, \quad (2)$$

in which η_{H} is the mass-accumulation efficiency for H-shell burning. The values of η_{H} are:

$$\eta_{\text{H}} = \begin{cases} \dot{M}_{\text{cr}}/|\dot{M}_2|, & |\dot{M}_2| > \dot{M}_{\text{cr}}, \\ 1, & \dot{M}_{\text{cr}} \geq |\dot{M}_2| \geq \dot{M}_{\text{low}}, \\ 0, & |\dot{M}_2| < \dot{M}_{\text{low}}. \end{cases} \quad (3)$$

He is assumed to be ignited when the mass of the He layer reaches a certain value.

The WD mass-growth rate, \dot{M}_{CO} , is defined as

$$\dot{M}_{\text{CO}} = \eta_{\text{He}} \dot{M}_{\text{He}} = \eta_{\text{He}} \eta_{\text{H}} |\dot{M}_2|, \quad (4)$$

in which η_{He} is the mass-accumulation efficiency for He-shell burning. The values of η_{He} are linearly interpolated from a grid, in which a wide range of WD masses and mass-transfer rates were calculated in the He-shell flashes (see Kato & Hachisu 2004). Note that the accumulation efficiencies used in this paper were derived for non-rotating WD models, but it is assumed that they are still valid for rotating WDs.²

The prescriptions above are incorporated into the Eggleton stellar evolution code, and the evolution of the WD + MS systems is followed. The mass lost from these WD binaries

² It has been suggested that rotation plays an important role on the accumulation efficiencies (see Piersanti et al. 2003). Especially, He burning has been found to be much less violent when rotation is taken into account (e.g. Yoon, Langer & Scheithauer 2004), which may significantly increase the He accretion efficiency.

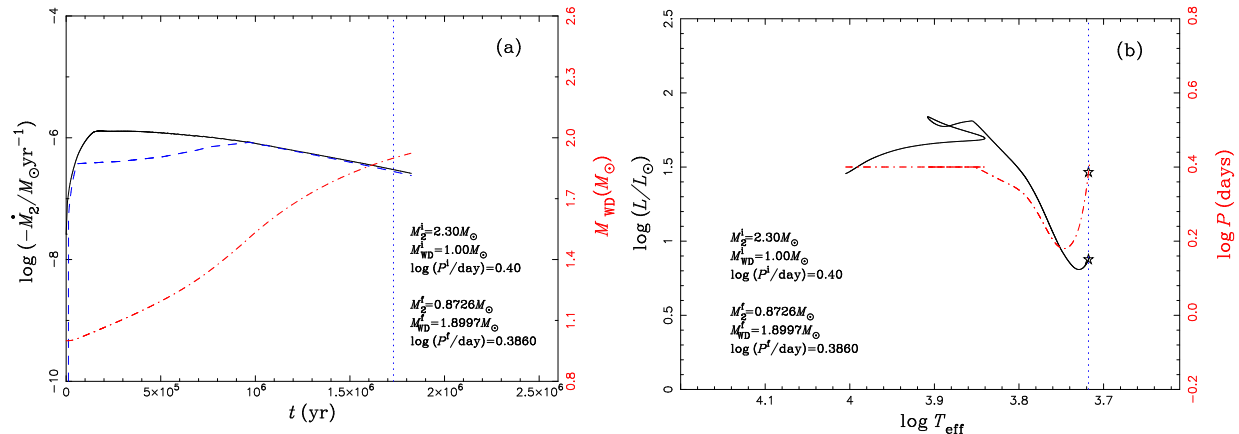


Figure 1. A representative example of binary evolution calculations. Panel (a): the evolution of the mass-transfer rate (solid curve), the mass-growth rate of the WD (dashed curve) and the mass of the WD (dash-dotted curve) as a function of time for the binary calculation. Panel (b): luminosity of the mass-donating star (solid curve, left-hand axis) and binary orbital period (dash-dotted curve, right-hand axis) as a function of effective temperature. Dotted vertical lines in both panels and asterisks in panel (b) indicate the position where the WD increases the mass to its maximum. The initial binary parameters and the parameters when the WD mass grows to its maximum are also given in these two panels.

is assumed to carry away the specific orbital angular momentum of the WD, whereas the mass loss induced by the donor’s wind is supposed to be negligible (e.g. Wang, Li & Han 2010). Finally, a large and dense model grids are obtained.

3 RESULTS OF BINARY EVOLUTION CALCULATIONS

In Fig. 1, we present a representative case of the binary evolution calculations. The WD explosion mass in this case is higher than $1.5 M_\odot$, i.e. a case in which the WD requires differential rotation to postpone explosion or collapse. The initial binary parameters are $(M_2^i, M_{\text{WD}}^i, \log(P^i/\text{day})) = (2.30, 1.00, 0.40)$, in which M_2^i , M_{WD}^i and P^i are the initial mass of the MS star and of the WD in solar masses, and the initial orbital period in days, respectively. In this case, the mass-donating star fills its Roche lobe in the subgiant stage, which results in early Case B mass transfer. The mass-transfer rate $|\dot{M}_2|$ exceeds \dot{M}_{cr} soon after the start of Roche-lobe overflow, leading to a wind phase in which a part of the transferred mass is blown off in the form of the optically thick wind, and the rest is accumulated onto the surface of the WD. After about 10^6 yr, $|\dot{M}_2|$ drops below \dot{M}_{cr} but remains higher than \dot{M}_{st} . Thus, the optically thick wind stops and the H-shell burning is stable. With the continuing decrease of $|\dot{M}_2|$, the system enters into a weak H-shell flash phase. The WD always grows in mass until the mass-transfer rate decreases to \dot{M}_r . At this moment, the mass of the WD is $M_{\text{WD}}^f = 1.8997 M_\odot$, the mass of the donor star is $M_2^f = 0.8726 M_\odot$, and the orbital period $\log(P^f/\text{day}) = 0.3860$.

Figs 2–5 show the final outcomes of our binary evolution calculations in the initial orbital period and secondary mass plane. The green triangles, blue circles and red squares denote that the WD explodes as a SN Ia with the WD mass in the range of $1.378 \leq M_{\text{WD}} < 1.5 M_\odot$, $1.5 \leq M_{\text{WD}} < 2.0 M_\odot$ and $M_{\text{WD}} \geq 2.0 M_\odot$, respectively. It is tempting to link WD explosion mass ranges with observed SN Ia subtypes. For example, “normal” SNe Ia might naturally be associated with the WD mass in the range of $1.378 \leq M_{\text{WD}} < 1.5 M_\odot$, which can be supported by solid-body rotation. The mass ranges displayed in our figures corresponding to the divisions chosen by Hachisu et al. (2012b). They associated the middle mass range ($1.5 \leq M_{\text{WD}} < 2.0 M_\odot$) with the brighter SN 1991T-like class, with the acknowledged super-Chandrasekhar events from yet more massive WDs ($M_{\text{WD}} \geq 2.0 M_\odot$). However, we note that

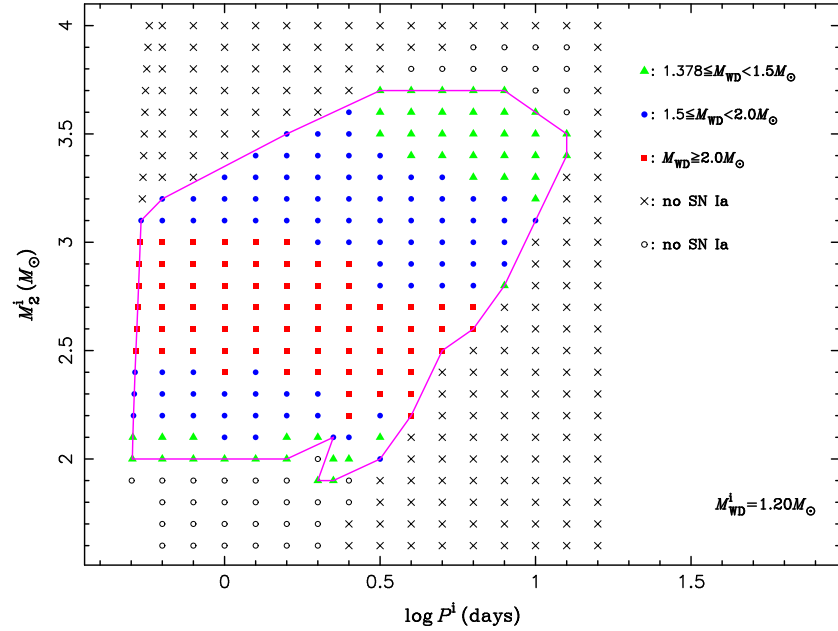


Figure 2. Final results of binary evolution calculations in the initial orbital period–secondary mass ($\log P^i$, M_2^i) plane of the WD + MS system for an initial WD mass of $1.2M_\odot$. The filled symbols represent systems resulting in a SN Ia explosion. The green triangles, blue circles and red squares denote WD explosion masses in the range of $1.378 \leq M_{\text{WD}} < 1.5M_\odot$, $1.5 \leq M_{\text{WD}} < 2.0M_\odot$, and $M_{\text{WD}} \geq 2.0M_\odot$, respectively. Open circles indicate systems that experience novae which prevent the WD from reaching $1.378M_\odot$, whereas crosses represent those which experience dynamically unstable mass transfer.

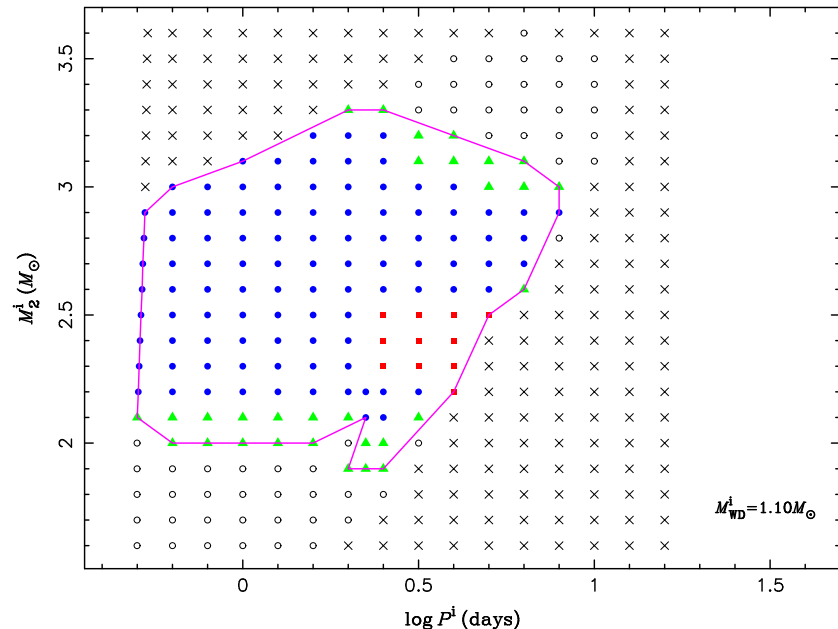


Figure 3. As Fig. 2, but for an initial WD mass of $1.1M_\odot$.

Mazzali et al. (2007) inferred a mass for the progenitor of a SN 1991T-like object which is consistent with the Chandrasekhar mass. For a discussion about the ranges of WD explosion mass see Section 6.1.

Some simulated WD + MS binaries fail to produce SNe Ia due to nova explosions that prevents the WD growing in mass to $1.378M_\odot$ (open circles in Figs 2–5), or dynamically unstable mass transfer (crosses in Figs 2–5). The maximum explosion mass of the WD in our calculations is $2.4558M_\odot$. We note that WDs supported by differential rotation might

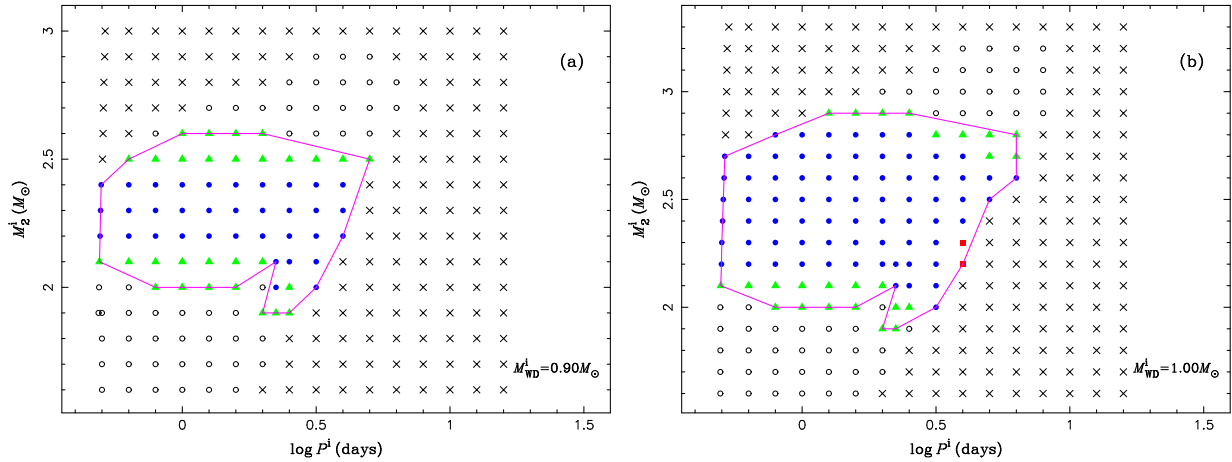


Figure 4. As Fig. 2, but for initial WD masses of 0.9 and $1.0 M_{\odot}$.

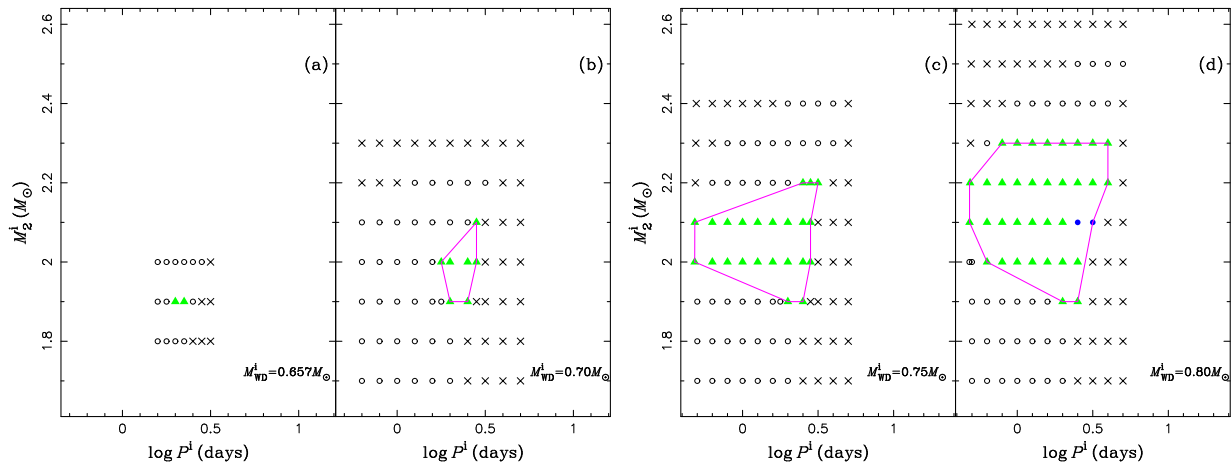


Figure 5. As Fig. 2, but for initial WD masses of 0.657, 0.70, 0.75 and $0.80 M_{\odot}$.

explode as SNe Ia soon after the WD mass exceeds $2.4 M_{\odot}$ due to a secular instability at $T/|W| \sim 0.14$, in which T and W are the rotational and gravitational energies of the WD, respectively (e.g. Yoon & Langer 2004; Hachisu et al. 2012a). At this point, the WD would be too massive to maintain hydrostatic equilibrium and would contract on a short timescale due to angular momentum redistribution. As a result of such rapid compression, carbon seems likely to be ignited in the central region of the WD, and then a SN Ia explosion might occur. Our binary evolution models predict that SNe Ia from this case are rare, since it only happens when $M_{\text{WD}}^i \geq 1.2 M_{\odot}$.

4 METHOD OF BINARY POPULATION SYNTHESIS

In order to obtain SN Ia birthrates and delay times, and the properties of the mass-donating star at the point when the WD increases the mass to its maximum, a series of Monte Carlo simulations in the BPS approach are performed. The following initial conditions for the Monte Carlo simulations are adopted: (1) The initial mass function of the primary star is from Miller & Scalo (1979). The mass of the primary star is from $0.1 M_{\odot}$ to $100 M_{\odot}$. (2) A constant mass-ratio distribution is taken (e.g. Goldberg & Mazeh 1994). (3) The distribution

of initial orbital separations is assumed to be constant in $\log a$ for wide binary systems, where a is orbital separation (e.g. Han, Podsiadlowski & Eggleton 1995). (4) A circular orbit is assumed for all binary systems. (5) A constant star formation rate (SFR) is simply assumed over the past 14 Gyr or, alternatively, as a delta function, i.e. a single instantaneous starburst (a burst producing $10^{10} M_{\odot}$ in stars is assumed). We intend the constant SFR to provide a rough description of spiral galaxies, and the delta function to approximate elliptical galaxies (or star clusters, for which the normalization would need to be altered).

For each BPS simulation, we employed the Hurley binary evolution code (Hurley, Pols & Tout 2002) to evolve 10^7 sample binaries. These binaries are followed from the star formation to the formation of the CO WD + MS systems based on three binary evolutionary scenarios (i.e. *He star*, *E-AGB* and *TP-AGB scenarios*; for details see Section 4.2 of Wang, Li & Han 2010). The metallicity in these simulations is set to be 0.02. If the initial parameters of a WD + MS system at the start of the Roche-lobe overflow are located in the SN Ia production regions in the plane of $(\log P^i, M_2^i)$ for its specific M_{WD}^i , a SN Ia is assumed to occur, and the properties of the WD + MS system when the WD increases the mass to its maximum are obtained by interpolation in the three-dimensional grid $(M_{\text{WD}}^i, M_2^i, \log P^i)$ of the WD + MS systems calculated in Section 3.

In the binary evolution, the WD + MS system is most likely produced from the common-envelope evolution of a giant binary system. Common-envelope evolution is still very poorly-understood (e.g. Ivanova et al. 2013; Zuo & Li 2014), so we use the standard energy equations to estimate the outcome of each common-envelope phase (e.g. Webbink 1984). In this parametrization of common-envelope evolution, there are two unknown parameters, i.e. α_{ce} and λ , in which α_{ce} is the ejection efficiency of common-envelope energy and λ is a stellar structure parameter that relates to the definition of the core-envelope boundary and the evolutionary stage of the mass-donating star. Similar to our previous works (e.g. Wang et al. 2009b), we used a single free parameter $\alpha_{\text{ce}}\lambda$ to describe the process of the common-envelope ejection, and gave the results for two specific values (i.e. 0.5 and 1.5).

5 RESULTS OF BINARY POPULATION SYNTHESIS

5.1 Birthrates and delay times of SNe Ia

The observed SN Ia birthrate in our Galaxy is $\sim 3 - 4 \times 10^{-3} \text{ yr}^{-1}$ (e.g. Cappellaro & Turatto 1997), which can be used to constrain the progenitor models of SNe Ia. In Fig. 6, we show the evolution of Galactic SN Ia birthrates from different ranges of WD explosion mass by adopting $Z = 0.02$ and $\text{SFR} = 5 M_{\odot} \text{ yr}^{-1}$. According to our standard model ($\alpha_{\text{ce}}\lambda = 0.5$) for the WD + MS channel, the simulation gives the Galactic total SN Ia birthrate of $\sim 1.36 \times 10^{-3} \text{ yr}^{-1}$ (black solid curve in Fig. 6). However, the birthrate from $\alpha_{\text{ce}}\lambda = 1.5$ is lower than that of $\alpha_{\text{ce}}\lambda = 0.5$; the simulation with $\alpha_{\text{ce}}\lambda = 1.5$ gives a total SN Ia birthrate of $\sim 1.05 \times 10^{-3} \text{ yr}^{-1}$ (black dashed curve in Fig. 6). This is because the binaries which result from common-envelope ejections tend to have slightly closer orbits for $\alpha_{\text{ce}}\lambda = 0.5$ and are therefore more likely to be located in the SN Ia production region. From this simulation, the birthrate of SNe Ia with WD explosion masses $\geq 2 M_{\odot}$ is $\sim 2.44 \times 10^{-5} \text{ yr}^{-1}$ based on our standard model, whereas the simulation with $\alpha_{\text{ce}}\lambda = 1.5$ does not produce these massive WDs. This is due to the lack of WDs with initial masses $\geq 1 M_{\odot}$ for the simulation of $\alpha_{\text{ce}}\lambda = 1.5$ (see Fig. 9).

The theoretical delay time distributions of SNe Ia can be compared with that of observations, and then used to examine current progenitor models (e.g. Mennekens et al. 2010; Meng & Yang 2010). In Fig. 7, we present the evolution of SN Ia birthrates for a single star-

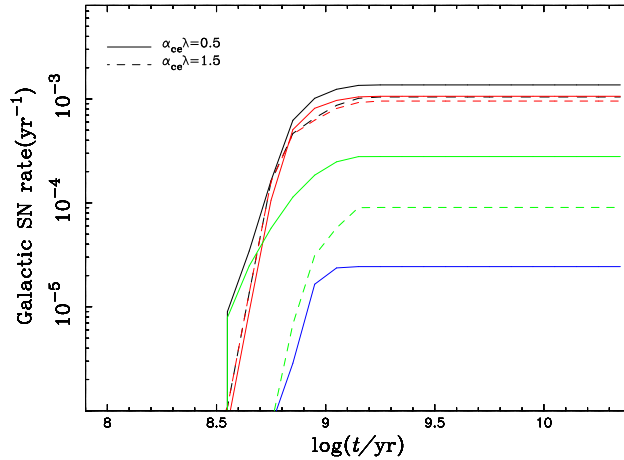


Figure 6. Evolution of Galactic SN Ia birthrates with time for a constant Population I SFR ($Z = 0.02$, $\text{SFR} = 5 M_{\odot} \text{yr}^{-1}$). The black curves are for the total SN Ia birthrates. The red, green and blue curves are for SNe Ia with WD explosion masses in the range of $1.378\text{--}1.5 M_{\odot}$, $1.5\text{--}2 M_{\odot}$ and $\geq 2 M_{\odot}$, respectively. The solid and dashed curves show the results of different common-envelope ejection parameters with $\alpha_{\text{ce}}\lambda = 0.5$ (solid) and $\alpha_{\text{ce}}\lambda = 1.5$ (dashed), respectively. Note that there is no blue dashed curve in this figure, for the reason see the text.

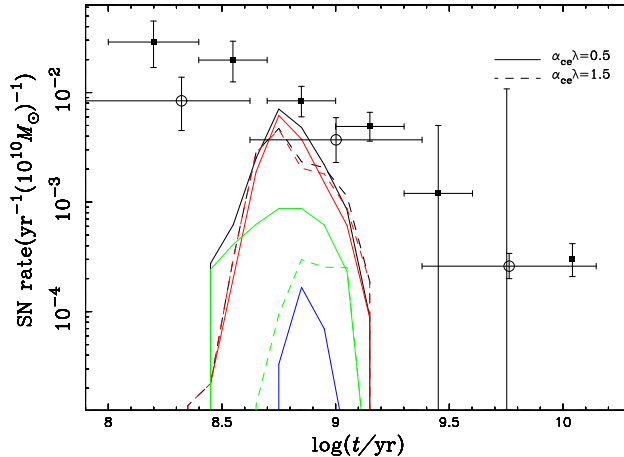


Figure 7. As Fig. 6, but for a single starburst with a total mass of $10^{10} M_{\odot}$. The open circles are from Maoz et al. (2011), and the filled squares from Totani et al. (2008).

burst with a total mass of $10^{10} M_{\odot}$. From this figure, we can see that a high value of $\alpha_{\text{ce}}\lambda$ leads to a systematically later explosion time for the WD + MS channel. This is because a high value of $\alpha_{\text{ce}}\lambda$ leads to wider WD binaries, and, as a consequence, it takes a longer time for the companion to fill its Roche lobe. This figure also shows that SN explosions from the WD + MS channel have delay times of $\sim 250 \text{ Myr} \text{--} 1.4 \text{ Gyr}$, which suggests that this channel only has a contribution to part of the overall SNe Ia. For other potential SN Ia production methods see Wang, Justham & Han (2013), Soker, García-Berro & Althaus (2014) and Meng & Podsiadlowski (2014).

Compared to some recent studies (e.g. Ruiter, Belczynski & Fryer 2009; Bours, Toonen & Nelemans 2013), we have obtained higher SN Ia birthrates for the WD + MS channel. The main difference is that they adopted the efficiency of mass accumulation on the surface of WDs from Prialnik & Kovetz (1995), which is significantly lower than that assumed in this work. However, the specific efficiency of mass accumulation is still uncertain (see Cassisi, Iben & Tornambè 1998).

After the WD accretes matter to reach the final explosion mass, the WD probably needs a spin-down time before it explodes (e.g. Justham 2011; Di Stefano, Voss & Claeys

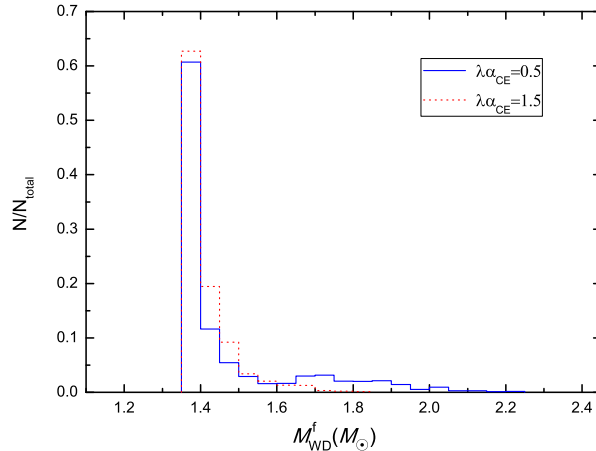


Figure 8. Distribution of WD explosion masses for the WD + MS channel with different values of $\alpha_{ce}\lambda$.

2011; Hachisu et al. 2012a,b). The time delay after the end of the mass transfer whilst the WD internally redistributes or loses spin angular momentum – “spins down” – may be the most natural way by which the SD model can satisfy observational constraints which would otherwise be problematic for it. However, the spin-down time is still uncertain. (1) For WDs which can be supported by rigid-body rotation, the spin-down time is mainly determined by angular momentum loss from the WD. In the absence of other braking mechanisms, this likely depends on the strength of the WD magnetic field, e.g. spin down may take more than 10^9 yr for magnetic fields of $\sim 10^6$ G (e.g. Ilkov & Soker 2011). (2) For WDs massive enough to require the support of differential rotation then, as angular momentum in the WD core is lost or redistributed toward rigid-body rotation, the WD core will contract until its central density and temperature become high enough to ignite carbon. Meng & Podsiadlowski (2013) recently argued that the upper limit of the spin-down timescale is a few 10^7 yr for SN Ia progenitor systems that contain a red giant donor. Note that the effect of spin-down time on the delay time distributions of SNe Ia is neglected in Fig. 7 due to the uncertainties of spin-down timescale.

5.2 Distribution of WD explosion masses

Fig. 8 shows the distribution of the WD explosion mass with different assumed values of $\alpha_{ce}\lambda$. The simulation predicts a range of WD explosion masses extending from 1.378 to $>2 M_{\odot}$. With $\alpha_{ce}\lambda = 0.5$, 77% of these exploding WDs are predicted to have masses in the range of 1.378 – $1.5 M_{\odot}$, i.e. to be WDs which can be supported by rigid-body rotation, 23% have progenitor masses $>1.5 M_{\odot}$ which require differential rotation for support (only 2% of the total in this study have WD explosion masses $\geq 2.0 M_{\odot}$; these SNe require the initial mass of the WD to be larger than $1.0 M_{\odot}$). Over-luminous events clearly form a relatively rare subclass of SNe Ia, and they have WD explosion mass more massive than $2.0 M_{\odot}$; about 1% SNe Ia can be of this type (e.g. Howell et al. 2006; Hicken et al. 2007; Scalzo et al. 2010; Silverman et al. 2011). If the WD + MS channel has a contribution to the total SNe Ia in the observations, the simulation from this work will occupy $\sim 2\%$ over-luminous events based on our standard model, which is comparable with that of observations. Additionally, a higher proportion of the SN Ia population comes from WDs which could be supported by

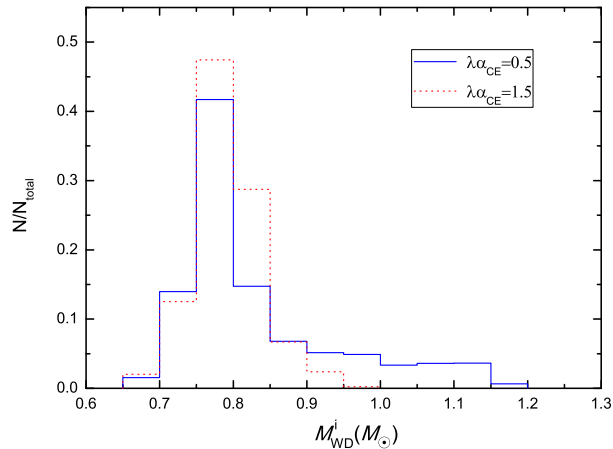


Figure 9. Distribution of the initial WD masses for WD + MS systems that ultimately produce SNe Ia with different values of $\alpha_{ce}\lambda$.

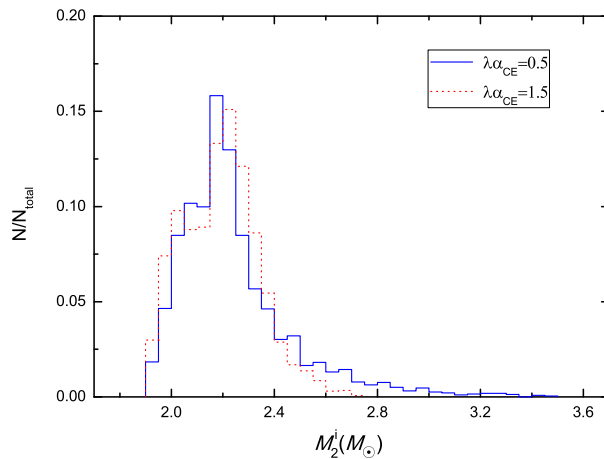


Figure 10. As Fig. 9, but for the distribution of the initial masses of secondaries in WD + MS systems.

rigid-body rotation until explosion when compared with previous work (for a discussion of this see Section 6.1).

5.3 Initial parameters of WD + MS systems

Some WD + MS systems are candidates to be SN Ia progenitors in the observations, for reviews see Wang & Han (2012) and Parthasarathy et al. (2007). According to our BPS calculations, we can present some properties of initial WD + MS systems for producing SNe Ia, which would be helpful to search potential progenitor candidates of SNe Ia.

Fig. 9 shows the distribution of initial WD masses in WD + MS systems that ultimately produce SNe Ia for different values of $\alpha_{ce}\lambda$. The solid and dotted histograms represent the cases with $\alpha_{ce}\lambda = 0.5$ and $\alpha_{ce}\lambda = 1.5$, respectively. The simulation uses a metallicity of $Z = 0.02$ and a constant initial mass-ratio distribution. This figure displays a result of the current epoch for a constant SFR. From this figure, we can see that the distribution for

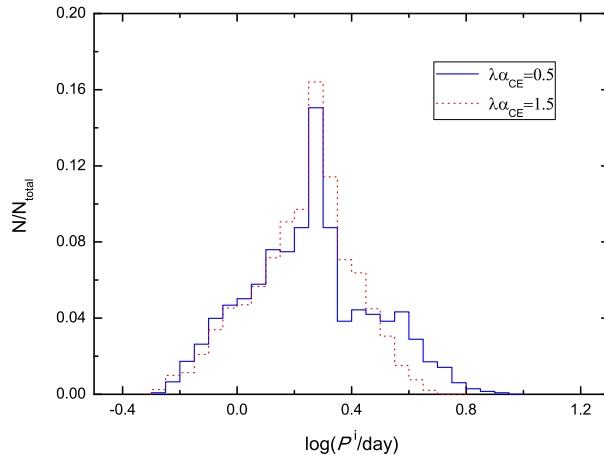


Figure 11. As Fig. 9, but for the distribution of the initial orbital periods of WD + MS systems.

$\alpha_{ce}\lambda = 0.5$ has a high-mass tail, but this does not appear in the case of $\alpha_{ce}\lambda = 1.5$. These massive CO WDs are mainly from *TP-AGB scenario* (see Section 4.2 of Wang, Li & Han 2010). Because of the low binding energy of the common envelope and the long primordial orbital period in the *TP-AGB scenario*, $\alpha_{ce}\lambda$ has a significant influence on the formation of the WD + MS systems; if a common envelope can be ejected, a low $\alpha_{ce}\lambda$ value produces a WD + MS system with shorter orbital period that is more likely to fulfil the conditions for producing SNe Ia. Thus, we can see obvious contributions from the *TP-AGB scenario* when $\alpha_{ce}\lambda = 0.5$, but very little contribution when $\alpha_{ce}\lambda = 1.5$.

Fig. 10 represents the distribution of the initial masses of secondaries in WD + MS systems for producing SNe Ia. From this figure, we can see that the distribution for $\alpha_{ce}\lambda = 0.5$ has a high-mass tail that is from the contribution of the *TP-AGB scenario*. In addition, a more massive secondary in a WD + MS system will evolve more quickly and thus produce a SN Ia at an earlier time. In Fig. 11, we display the distribution of the initial orbital periods of WD + MS systems for the production of SNe Ia. Similar to the distributions of the initial masses of CO WDs and those of the initial orbital periods, the long orbital periods for $\alpha_{ce}\lambda = 0.5$ are also from the *TP-AGB scenario*.

6 DISCUSSION

6.1 WD explosion mass

The WDs with masses that could be supported by rigid-body rotation until explosion from Hachisu et al. (2012b) account for 48% of the total.³ However, the result from our calculations is 77%. The main difference is that they did not employ full stellar evolution calculations; they adopted a simple analytical fitting formulae for estimating the mass-transfer rate (for details see Section 5.1 of Han & Podsiadlowski 2004). Specifically, the minimum initial WD mass for producing SNe Ia from Hachisu et al. (2012b) is about $0.7 M_{\odot}$, but only few SNe Ia are obtained from this WD mass due to very small region for producing SNe Ia. However, we obtained more SNe Ia for low-mass initial WDs, which have a higher contribution to SN Ia population that could be supported by rigid-body rotation. Our substantially higher fraction

³ Hachisu et al. (2012b) did not employ detailed BPS calculations to obtain this value.

of WDs with explosion masses of $1.5 M_{\odot}$ or less should be helpful with reconciling these SD SNe Ia with the inference that most SNe Ia have masses close to the Chandrasekhar mass (Mazzali et al. 2007).

Hachisu et al. (2012b) have chosen to map the observed subtypes of SNe Ia onto the full range of the WD explosion masses. They associated the rigid-body rotation population ($1.378\text{--}1.5 M_{\odot}$) with “normal” SNe Ia and 91bg-like events, and the differential rotation population ($>1.5 M_{\odot}$) with the brighter 91T-like class and over-luminous events. However, the work by Mazzali et al. (2007) concludes that the pre-explosion WD masses of a diverse sample of SNe Ia is consistent with the Chandrasekhar mass, in which the sample includes 91bg-like, spectroscopically normal and 91T-like events. Without a systematic bias in either method or sample of events, their results suggest that it is unlikely that the class of 91T-like SNe includes events with pre-explosion masses as high as $2 M_{\odot}$, as adopted by Hachisu et al. (2012b). Even so, we note that an updated analysis of 91bg-like events by Mazzali & Hachinger (2012) does allow the progenitor masses for this class of SNe Ia to be lower than the masses indicated by the study of Mazzali et al. (2007). Interestingly, the work by Mazzali et al. (2007) indicates that the normal range of SNe Ia arises from WD masses which are low enough to be supported by near solid-body rotation (i.e. within $\approx 0.1 M_{\odot}$ of the normally-assumed ignition mass, $1.378 M_{\odot}$).

Justham (2011) suggested that future BPS calculations should investigate to what extent typical WD masses in SD SNe Ia would exceed the Chandrasekhar mass if the spin of the accreting WD delays the explosion. This work has investigated that question. For the standard assumptions in our model, most WDs (77%) have low enough masses to be supported by solid-body rotation. This helps to support the spin-up/spin-down scenario as a viable explanation for the lack of H in SNe Ia if they are produced from SD progenitor systems.

6.2 Post-accretion system appearance and post-explosion remnant properties

One of the most exciting possibilities arising from including the spin-down time of WDs in SD SN Ia models is that we would, in principle, be able to observe systems in which the WD is already more massive than M_{Ch} . In some cases, the WD would no longer be accreting; it would be losing or internally redistributing angular momentum whilst waiting to explode. We may have already known such systems. For example, in U Scorpii, the uncertainty in the dynamical mass measurement would allow the WD to be more massive than M_{Ch} (e.g. Thoroughgood et al. 2001). The novae RS Ophiuchi and V445 Puppis are each also inferred to contain a WD with a mass very close to the Chandrasekhar limit, see Sokoloski et al. (2006) and Kato et al. (2008), respectively.

The mass-donating star in the SD model would survive after the SN explosion and potentially be identifiable soon after the WD is disrupted (e.g. Justham et al. 2009; Wang & Han 2009, 2010; Liu et al. 2012, 2013; Pan, Ricker & Taam 2014). The BPS gives current-epoch distributions of many properties of companions when the WD increases the mass to its maximum (e.g. the orbital velocities, the luminosities, the surface gravities, the effective temperatures, the surface abundances, etc). These properties may be a starting point to study the surviving companion stars of SNe Ia.

Fig. 12 shows an example of the distributions of the properties of companion stars in the orbital velocity and companion mass plane at the point when the WD mass has increased to its maximum, which may be helpful for identifying the surviving companions. The star known as Tycho G was suggested to be a possible surviving companion star from the system which produced Tycho’s SN (a Galactic SN Ia) by Ruiz-Lapuente et al. (2004). They found

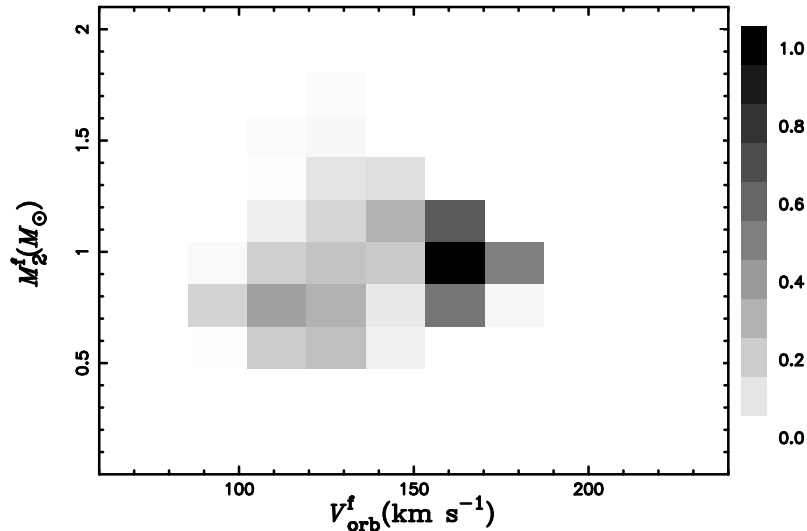


Figure 12. The distribution of properties of the companions in the plane of $(V_{\text{orb}}^f, M_2^f)$ at the current epoch, in which V_{orb}^f is the orbital velocity and M_2^f the companion mass when the WD mass reaches its maximum. Here, we set $\alpha_{\text{ce}\lambda} = 0.5$.

that this star have a spatial velocity of 136 km/s that is more than three times the mean velocity of the stars in the vicinity. This velocity is compatible with the value obtained from this study. However, whether Tycho G is the surviving companion of Tycho’s SN is still debatable (see, e.g. Fuhrmann 2005; Kerzendorf et al. 2009, who found no evidence that Tycho G has an anomalous space velocity). Additionally, the final properties of the surviving companions also depend on the spin-down time of WDs. If the spin-down time is long enough (e.g. $\sim 10^9$ yr), the companion will evolve to a He WD or CO WD when SN explosion occurs. In such case, any prominent signature of the companion is not expected immediately before or after the SN explosion (e.g. Justham 2011; Di Stefano, Voss & Claeys 2011).

6.3 SNe Ia with circumstellar material and apparent SNe IIn

The population of SN Ia progenitors in which the WD must be supported by differential rotation contains systems which might naturally produce a signature of H in SNe Ia. The mass-donating stars in these systems could still have substantial H envelope masses at SN explosion. In many cases, the WDs could still be accreting at a high mass-transfer rate at the moment of the explosion – or would have very recently been doing so – and would therefore be surrounded by dense, H-rich, circumstellar material. These systems might therefore help to explain two different phenomena. Firstly, it is now widely recognized that some SNe Ia (e.g. SN 2002ic-like objects) contain H at the moment of explosion although other models exist to explain these events (see, e.g. Hamuy et al. 2003; Livio & Riess 2003; Chugai & Yungelson 2004; Han & Podsiadlowski 2006; Wood-Vasey & Sokoloski 2006; Dilday et al. 2012). Secondly, and less well known, observational evidence has been increasing which indicates that a large fraction of the events classified as type IIn supernovae (SNe IIn) are not produced by massive stars (e.g. Kotak et al. 2004; Anderson et al. 2012), and a natural candidate to explain some of these events would be SNe Ia which explode inside a dense H-rich environment.

It is therefore not a new idea that some SNe which exhibit SN IIn phenomenology might be disguised SNe Ia. However, we suggest that many SNe which exhibit SN IIn phenomenology might be produced by explosions of WDs that had been supported by differential rotation, and that consequently the progenitor systems were H-rich at the time of SN explosion.

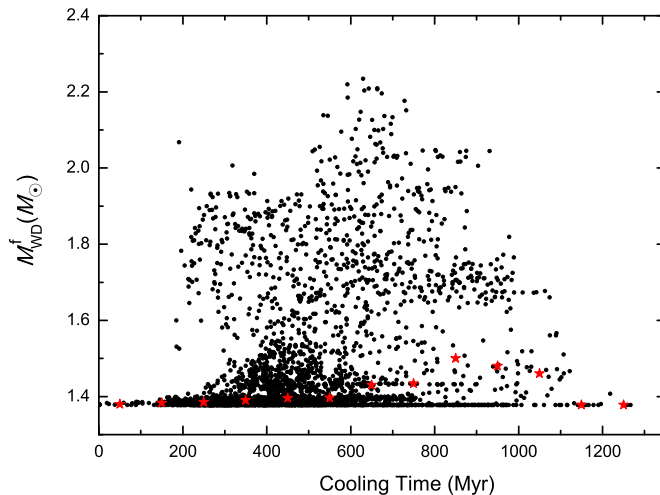


Figure 13. WD explosion mass versus WD cooling time before mass accretion, in which we set $\alpha_{ce}\lambda = 0.5$. The black circles denote the WD explosion mass versus WD cooling time for individual instances produced by our Monte-Carlo population synthesis. The red stars present the median WD explosion mass versus WD cooling time; these indicate that the majority of the SNe have explosion masses close to the Chandrasekhar mass.

If all WDs that could be supported by differential rotation have a contribution to SNe IIn, the birthrates from this scenario are $\sim 0.31 \times 10^{-3} \text{ yr}^{-1}$ based on our standard model. Unfortunately, the birthrates of SNe IIn are very uncertain, but some observational estimates give $\sim 0.13 - 1.22 \times 10^{-3} \text{ yr}^{-1}$ (Cappellaro & Turatto 1997; Smartt et al. 2009). Therefore, this scenario might produce a significant part of the population of SNe classified as type IIn. In this case then the WD masses of such disguised SNe Ia would be higher than those of typical SNe Ia; if those WD masses can be inferred, then it would provide a test of this model. We note that there is no H in observed over-luminous events, so the estimated birthrate for these SNe will become lower if the WD ($\geq 2.0 M_{\odot}$) is still accreting matter with a high mass-transfer rate at the moment of SN explosion.

6.4 SN Ia diversity

The overall origin of SN Ia systematic diversity is probably complex. We stress that we are not trying to explain the differences between individual SN Ia, but to explore reasons why different stellar populations show systematic differences in the SNe Ia which they produce. To first order, it is expected that the ^{56}Ni mass produced by each SN Ia controls the maximum luminosity (Arnett 1982), but the origin of the variation of the ^{56}Ni mass for different individual SN Ia is still uncertain (one possibility is the location of the deflagration-to-detonation transition; see also the Introduction).⁴ Whilst it is expected to be possible to have a wide variation in ^{56}Ni mass produced by identical WD explosion masses, it is obvious that differences in WD explosion mass may have an influence on ^{56}Ni masses in SNe Ia. If there were systematic population variations in WD masses with age, this might help to explain recent observations which find variations in SN Ia population properties with the age of the host stellar population (see, e.g. Howell et al. 2009; Pan et al. 2014).

⁴ Metallicity may also affect the appearance of SNe Ia (see Höflich, Wheeler & Thielemann 1998; Domínguez et al. 2001; Timmes, Brown & Truran 2003; Podsiadlowski et al. 2006; Bravo et al. 2010; Sullivan et al. 2010; Childress et al. 2013; Pan et al. 2014).

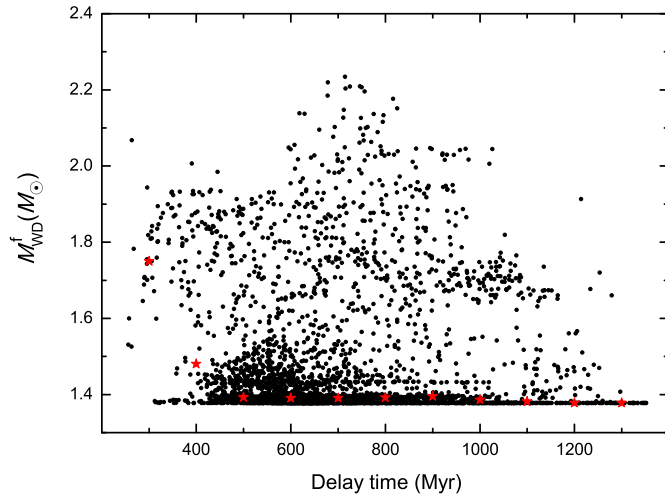


Figure 14. As Fig. 13, but for WD explosion mass versus SN Ia delay time. We stress that these delay times do not include any contribution from spin-down times. Note that for a delay time of 300 Myr the median WD explosion mass is significantly above $1.5 M_{\odot}$.

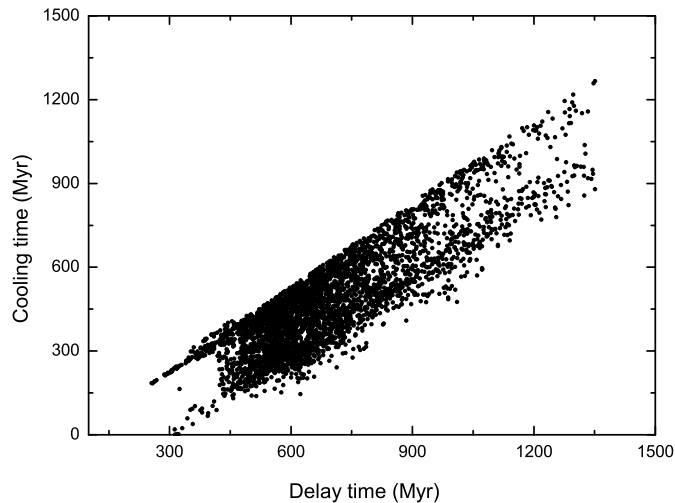


Figure 15. WD cooling time before mass accretion versus the delay time of SNe Ia, in which we set $\alpha_{ce}\lambda = 0.5$.

Not only should accounting for the accreting WD's spin angular momentum result in a range of WD masses at explosion, but it should also lead to a range of post-accretion cooling times before SN explosion due to the duration of the phase of spin-down or internal angular momentum redistribution (see also Hachisu et al. 2012a). In addition to this post-accretion cooling time, the pre-accretion cooling times also affect the material properties of the WD at explosion, in particular the density at SN explosion that may be the origin of the maximum luminosity scatter (e.g. Lesaffre et al. 2006; Krueger et al. 2010). WDs tend to crystallize after being cooled to a certain extent, which results in both a release of latent heat and gravitational energy, the former being a result of the phase separation of carbon and oxygen (e.g. García-Berro et al. 2000, 2011; Isern et al. 2000). This release of latent

heat and gravitational energy should induce a cooling time delay, leading to higher ignition densities (e.g. Lesaffre et al. 2006).

In Fig. 13, we show the distribution of WD explosion mass versus WD cooling time before mass accretion. From this figure it is clear that, for equivalent WD explosion masses, there can exist a wide range of pre-accretion cooling times. Interestingly, we find a systematic change in the distribution of median WD explosion masses for different cooling times (see the red stars in this figure), in which the peak of the median WD explosion mass is at relatively *long* cooling times. In Fig. 14, we present the distribution of WD explosion mass versus the delay time of SNe Ia that is corresponding to population age at the time of the SN explosion. Only in young populations is the median WD explosion mass significantly in excess of the Chandrasekhar mass, with a median explosion mass above $1.7 M_{\odot}$ for a delay time of 300 Myr. The explosions from the highest-mass WDs occur at intermediate ages, with a clear decrease in the frequency of high-mass explosions at late times (reminiscent of, e.g. Fig. 8 of Howell et al. 2009). Note that the delay times in Fig. 14 neglect the potentially long spin-down time for WDs in solid-body rotation. In Fig. 15, we show the WD cooling time before mass accretion versus SN Ia delay time. The SNe with long delay times are naturally correlated with long cooling times of WDs. Both the delay time and WD cooling time are both related to the mass of the MS star; a low-mass MS star takes a long evolutionary time to fill its Roche lobe, resulting in a long WD cooling time and a long delay time (see also Meng, Yang & Li 2010). However, the differences in the distributions of median WD masses in Figs 13–14 demonstrate that this is not a trivial relationship, presumably because *some* WDs with short cooling times explode after relatively long delay times, i.e. the formation of the WD was fine-tuned to the time of Roche-lobe filling.

We have shown that, if we allow mass accretion to delay the explosion of the WD, but for otherwise standard assumptions, most SD SN Ia progenitor systems still produce WDs which have masses at explosion sufficiently close to the canonical Chandrasekhar limit for them to avoid explosion whilst remaining in solid-body rotation. Some systematic diversity may arise from the pre-explosion cooling, as above. In addition, since a very wide-range of spin-down times seems to be a priori reasonable for these systems then, in principle, this narrow mass range of systems could produce a diverse range of SNe Ia, especially if some such WDs are able to crystallize before they explode. However, since the model predicts that the majority of SN Ia progenitors fall in this solid-body regime, and since most SNe Ia are inferred to have masses close to the Chandrasekhar mass (e.g. Mazzali et al. 2007), we strongly expect that the “normal” range of SNe Ia emerges from within this set of progenitors. Unfortunately, we cannot accurately predict the variation of explosion masses for the population of WDs in solid-body rotation. However, we expect that this accounts for at least some of the observed scatter, and very likely some of the observed systematic diversity. Note that Domínguez et al. (2006) has already explored the explosion of solid-body rotating WDs (up to $1.5 M_{\odot}$).

Clearly the extreme “super-Chandrasekhar” SNe Ia must, if they have SD progenitors, be supported by differential rotation before explosion. Assuming that the timescale of the angular momentum redistribution is not unexpectedly long, post-accretion cooling times seem unlikely to affect the diversity of the explosions produced by this set of differentially-rotating WDs. Here, systematic brightness diversity might be related with the wide range of final WD masses predicted by the model. Note also that the distribution of internal angular-momentum distributions at explosion (and therefore any dynamo-generated magnetic fields) should be correlated with WD mass.

7 SUMMARY

We have performed detailed binary evolution calculations of the WD + MS channel for the formation of SNe Ia. In an improvement over our previous works, we have allowed the WD to exceed the Chandrasekhar mass due to the accretion of angular momentum. We then combined these results with our BPS code to provide estimates for the population of SN Ia birthrates and delay times, along with the properties of the systems at explosion. The Galactic SN Ia birthrates from this work are $\sim 1.36 \times 10^{-3} \text{ yr}^{-1}$ based on our standard model, and the delay times are $\sim 250 \text{ Myr} - 1.4 \text{ Gyr}$. The birthrates from Hachisu et al. (2012b) are higher than those of this work due to a different method adopted.⁵

For our standard model, we find that 77% SNe Ia have WD explosion masses in the range of $1.378 - 1.5 M_{\odot}$, which is approximately the range of WD masses for which solid-body rotation is, in principle, able to delay the explosion of the WD. For WDs with initial mass $< 0.9 M_{\odot}$, all of the final WD masses are predicted to be below $1.5 M_{\odot}$. This high fraction of WDs which are predicted to end their accretion phase with masses $\leq 1.5 M_{\odot}$ supports the suggestion by Justham (2011) that accounting for the spin of the WD might enable the majority of SD SN Ia progenitors to avoid showing signs of H contamination (see also Di Stefano, Voss & Claeys 2011). In contrast to Hachisu et al. (2012b), we are able to accommodate the population of 91T-like SNe Ia within the set of WDs which explode with masses $\leq 1.5 M_{\odot}$. Some of the diversity of SN Ia explosion properties might be explained within this range of WD explosion masses, and the WD spin-down time before SN explosion is also expected to cause the diversity. Systematic correlations between population age and SN Ia luminosity might also be partly explained by a combination of both pre- and post-accretion cooling times.

Some models for the observed extremely luminous SNe Ia invoke the explosion of WDs with masses far in excess of the Chandrasekhar mass (of $\sim 2.0 M_{\odot}$ or more). Whilst our assumptions about accretion efficiency may be less reliable in this regime, our prediction is that 2% of SNe Ia from the WD + MS channel occur with masses $\geq 2.0 M_{\odot}$, which is broadly comparable with the inferred rate of these SNe. The proportion from Hachisu et al. (2012b) is 3.8% that is about two times of ours, but they have a small fraction with WD explosion masses $\leq 1.5 M_{\odot}$ (for the reason see Section 6.1).

For the 23% of systems which the model predicts to explode with WD masses $> 1.5 M_{\odot}$, we note that the fact that they need to be supported by differential rotation means that the explosion may well occur when the WD still has a H-rich companion, and in systems where the mass transfer is still ongoing. This assumes that internal angular momentum redistribution is relatively rapid, which is broadly expected. The work of Saio & Nomoto (2004) indicates that the timescale of angular momentum redistribution could be extremely short as the angular momentum transport is very fast (see also Piro 2008).⁶ We therefore suggest that these systems may help to explain the existence of SNe Ia with circumstellar material. In extreme cases, they might also contribute to the population of type IIn SNe.

If any SD scenario is correct, then the mass-donating star in the SD model would survive after the SN explosion, in which case our models may be useful for constraining the searches for remnant donors. If the spin-up/spin-down model is the correct scenario for SD SNe Ia, then some pre-explosion SN progenitor systems should be observable which contain rapidly-rotating WDs in excess of the Chandrasekhar mass. These could be systems which are

⁵ Hachisu et al. (2012b) used Equation (1) of Iben & Tutukov (1984) to estimate the birthrate of SNe Ia. However, Wang et al. (2009b) found that the SN Ia birthrate can be overestimated by this method.

⁶ The upper limits for the angular momentum redistribution time might be $\sim 10^8 \text{ yr}$ owing to angular momentum transport by the Eddington-Sweet meridional circulation (see Yoon & Langer 2004; Hachisu et al. 2012a).

continuing to accrete, with properties similar to those, as noted by Hachisu et al. (2012b), of U Scorpii, RS Ophiuchi and V445 Puppis. Alternatively, they could be post-accretion systems in which the WD is spinning down. We hope that observers will find such post-accretion systems, e.g. to find some binaries with massive WDs that are close to or above the Chandrasekhar mass, which would provide outstanding constraints on our understanding of SN Ia progenitors.

ACKNOWLEDGMENTS

We acknowledge the anonymous referee for valuable comments that helped us to improve the paper. We thank Paolo Mazzali for discussions about the Zorro diagram and inferring WD pre-explosion masses. We also thank Philipp Podsiadlowski, Xiangdong Li, Sung-Chul Yoon, Xiangcun Meng and Xuefei Chen for their helpful discussions. This work is supported by the National Basic Research Program of China (No. 2014CB845700), the National Natural Science Foundation of China (Nos. 11322327, 11103072, 11033008, 11390374, 11250110055 and 11350110324), and the Natural Science Foundation of Yunnan Province (Nos. 2013FB083 and 2013HB097).

REFERENCES

- Ablimit I., Xu X.-J., Li X.-D., 2014, *ApJ*, 780, 80
Anand S. P. S., 1965, *PNAS*, 54, 23
Anderson J. P., Haberman S. M., James P. A., Hamuy M., 2012, *MNRAS*, 424, 1372
Arnett W. D., 1982, *ApJ*, 253, 785
Bours M. C. P., Toonen S., Nelemans G., 2013, *A&A*, 552, A24
Bravo E., Domínguez I., Badenes C., Piersanti L., Straniero O., 2010, *ApJ*, 711, L66
Cappellaro E., Turatto M., 1997, in *Thermonuclear Supernovae*, ed. P. Ruiz-Lapuente, R. Cannal, & J. Isern (Dordrecht: Kluwer), 77
Cassisi S., Iben I., Tornambè A., 1998, *ApJ*, 496, 376
Chen W.-C., Li X.-D., 2009, *ApJ*, 702, 686
Chen X., Han Z., Meng X., 2014, *MNRAS*, 438, 3358
Chen X., Jeffery C. S., Zhang X., Han Z., 2012, *ApJ*, 755, L9
Childress M. et al., 2013, *ApJ*, 770, 108
Chugai N. N., Yungelson L. R., 2004, *Astronomy Letters*, 30, 65
Claeys J. S. W., Pols O. R., Izzard R. G., Vink J., Verbunt F. W. M., 2014, *A&A*, 563, A83
Di Stefano R., Voss R., Claeys J. S. W., 2011, *ApJ*, 738, L1
Dilday B. et al., 2012, *Science*, 337, 942
Domínguez I., Höflich P., Straniero O., 2001, *ApJ*, 557, 279
Domínguez I., Piersanti L., Bravo E., Tornambé A., Straniero O., Gagliardi S., 2006, 644, 21
Eggleton P. P., 1973, *MNRAS*, 163, 279
Eggleton P. P., Kiseleva-Eggleton L., 2002, *ApJ*, 575, 461
Fuhrmann K., 2005, *MNRAS*, 359, L35
García-Berro E. et al., 2010, *Nature*, 465, 194
García-Berro E., Torres S., Renedo I., Camacho J., Althaus L. G., Córscico A. H., Salaris M., Isern J., 2011, *A&A*, 533, A31
Goldberg D., Mazeh T., 1994, *A&A*, 282, 801

- Hachinger S. et al., 2012, MNRAS, 427, 2057
Hachisu I., 1986, ApJS, 61, 479
Hachisu I., Kato M., Nomoto K., 1996, ApJ, 470, L97
Hachisu I., Kato M., Nomoto K., Umeda H., 1999, ApJ, 519, 314
Hachisu I., Kato M., Saio H., Nomoto K., 2012a, ApJ, 744, 69
Hachisu I., Kato M., Nomoto K., 2012b, ApJ, 756, L4
Hamuy M. et al., 2003, Nature, 424, 651
Han Z., Podsiadlowski Ph., 2004, MNRAS, 350, 1301
Han Z., Podsiadlowski Ph., 2006, MNRAS, 368, 1095
Han Z., Podsiadlowski Ph., Eggleton P. P., 1994, MNRAS, 270, 121
Han Z., Podsiadlowski Ph., Eggleton P. P., 1995, MNRAS, 272, 800
Han Z., Tout C. A., Eggleton P. P., 2000, MNRAS, 319, 215
Hicken M. et al., 2007, ApJ, 669, L17
Hillebrandt W., Niemeyer J. C., 2000, ARA&A, 38, 191
Hillebrandt W., Sim S. A., Röpke F. K., 2007, A&A, 465, L17
Höflich P., Wheeler J. C., Thielemann F. K., 1998, ApJ, 495, 617
Howell D. A., 2011, Nature Communications, 2, 350
Howell D. A. et al., 2006, Nature, 443, 308
Howell D. A. et al., 2009, ApJ, 691, 661
Hurley J. R., Tout C. A., Pols O. R., 2002, MNRAS, 329, 897
Iben I., Tutukov A. V., 1984, ApJS, 54, 335
Idan I., Shaviv N. J., Shaviv G., 2012, Journal of Physics: Conference Series, 337, 012051
Ilkov M., Soker N., 2011, MNRAS, 419, 1695
Isern J., García-Berro E., Hernanz M., Chabrier G., 2000, ApJ, 528, 397
Ivanova N., Justham S., Avendano Nandez J. L., Lombardi J. C., 2013, Science, 339, 433
Justham, S. 2011, ApJ, 730, L34
Justham S., Wolf C., Podsiadlowski P., Han Z., 2009, A&A, 493, 1081
Kasen D., Röpke F. K., Woosley S. E., 2009, Nature, 460, 869
Kato M., Hachisu I., 2004, ApJ, 613, L129
Kato M., Hachisu I., Kiyota S., Saio H., 2008, ApJ, 684, 1366
Kerzendorf W. E. et al., 2009, ApJ, 701, 1665
Kotak R., Meikle W. P. S., Adamson A., Leggett S. K., 2004, MNRAS, 354, L13
Krueger B. K. et al., 2010, ApJ, 719, L5
Langer N., Deutschmann A., Wellstein S., Höflich P., 2000, A&A, 362, 1046
Lesaffre P., Han Z., Tout C. A., Podsiadlowski Ph., Martin R. G., 2006, MNRAS, 368, 187
Li X.-D., van den Heuvel E. P. J., 1997, A&A, 322, L9
Liu Z.-W. et al., 2012, A&A, 548, A2
Liu Z.-W. et al., 2013, A&A, 554, A109
Livio M., Riess A. G., 2003, ApJ, 594, L93
Livio M., Soker N., 1988, ApJ, 329, 764
Lü G., Zhu C., Wang Z., Wang N., 2009, MNRAS, 396, 1086
Maeda K. et al., 2010, Nature, 466, 82
Maoz D., Mannucci F., Li W., Filippenko A. V., Della Valle M., Panagia N., 2011, MNRAS, 412, 1508
Maoz D., Mannucci F., Nelemans G., 2014, ARA&A, 52, 107
Mazzali P. A., Hachinger S., 2012, MNRAS, 424, 2926
Mazzali P. A., Röpke F. K., Benetti S., Hillebrandt W., 2007, Science, 315, 825
Meng X., Chen X., Han Z., 2009, MNRAS, 395, 2103
Meng X., Podsiadlowski P., 2013, ApJ, 778, L35

- Meng X., Podsiadlowski P., 2014, *ApJ*, 789, L45
- Meng X., Yang W., 2010, *ApJ*, 710, 1310
- Meng X., Yang W., Li Z., 2010, *Res. Astron. Astrophys.*, 10, 927
- Mennekens N., Vanbeveren D., De Greve J. P., De Donder E., 2010, *A&A*, 515, A89
- Miller G. E., Scalo J. M., 1979, *ApJS*, 41, 513
- Nelemans G., Yungelson L. R., Portegies Zwart S. F., Verbunt F., 2001, *A&A*, 365, 491
- Nelson C. A., Eggleton P. P., 2001, *ApJ*, 552, 664
- Newsham G., Starrfield S., Timmes F., 2013, preprint (arXiv:1303.3642)
- Nomoto K., Iwamoto K., Kishimoto N., 1997, *Science*, 276, 1378
- Ostriker J. P., Bodenheimer P., 1968, *ApJ*, 151, 1089
- Pan K.-C., Ricker P. M., Taam R. E., 2014, *ApJ*, 792, 71
- Pan Y.-C. et al., 2014, *MNRAS*, 438, 1391
- Parrent J., Friesen B., Parthasarathy M., 2014, *Ap&SS*, 351, 1
- Parthasarathy M., Branch D., Jeffery D. J., Baron E., 2007, *New Astron. Rev.*, 51, 524
- Perlmutter S. et al., 1999, *ApJ*, 517, 565
- Piersanti L., Gagliardi S., Iben I., Tornambé A., 2003, *ApJ*, 598, 1229
- Piro A. L., 2008, *ApJ*, 679, 616
- Podsiadlowski P., Mazzali P., Lesaffre P., Han Z., Förster F., 2008, *New Astro. Rev.*, 52, 381
- Podsiadlowski P., Mazzali P., Lesaffre P., Wolf C., Förster F., 2006, astro-ph/0608324
- Pols O. R., Schröder K. P., Hurly J. R., Tout C. A., Eggleton P. P., 1998, *MNRAS*, 298, 525
- Pols O. R., Tout C. A., Eggleton P. P., Han Z., 1995, *MNRAS*, 274, 964
- Pols O. R., Tout C. A., Schröder K. P., Eggleton P. P., Manners, J., 1997, *MNRAS*, 289, 869
- Prialnik D., Kovetz A., 1995, *ApJ*, 445, 789
- Riess A. et al., 1998, *AJ*, 116, 1009
- Röpke F. K., Hillebrandt W., 2004, *A&A*, 420, L1
- Ruiter A. J., Belczynski K., Fryer C. L., 2009, *ApJ*, 699, 2026
- Ruiz-Lapuente P. et al., 2004, *Nature*, 431, 1069
- Saio H., Nomoto K., 2004, *ApJ*, 615, 444
- Scalzo R. A. et al., 2010, *ApJ*, 713, 1073
- Silverman J. M. et al., 2011, *MNRAS*, 410, 585
- Smartt S. J., Eldridge J. J., Crockett R. M., Maund J. R., 2009, *MNRAS*, 395, 1409
- Soker N., García-Berro E., Althaus L. G., 2014, *MNRAS*, 437, L66
- Sokoloski J. L., Luna G. J. M., Mukai K., Kenyon S. J., 2006, *Nature*, 442, 276
- Sullivan M. et al., 2010, *MNRAS*, 406, 782
- Thoroughgood T. D., Dhillon V. S., Littlefair S. P., Marsh T. R., Smith D. A., 2001, *MNRAS*, 327, 1323
- Timmes F. X., Brown E. F., Truran J. W., 2003, *ApJ*, 590, L83
- Toonen S., Nelemans G., Portegies Zwart S., 2012, *A&A*, 546, A70
- Totani T., Morokuma T., Oda T., Doi M., Yasuda, N., 2008, *PASJ*, 60, 1327
- Uenishi T., Nomoto K., Hachisu I., 2003, *ApJ*, 595, 1094
- van Kerkwijk M. H., Chang P., Justham S., 2010, *ApJ*, 722, L157
- Wang B., Han Z., 2009, *A&A*, 508, L27
- Wang B., Han Z., 2010, *MNRAS*, 404, L84
- Wang B., Han Z., 2012, *New Astron. Rev.*, 56, 122
- Wang B., Justham S., Han Z., 2013, *A&A*, 559, A94
- Wang B., Li X.-D., Han Z., 2010, *MNRAS*, 401, 2729

- Wang B., Meng X., Chen X., Han Z., 2009a, MNRAS, 395, 847
Wang B., Chen X., Meng X., Han Z., 2009b, ApJ, 701, 1540
Wang L., Wheeler J. C., 2008, ARA&A, 46, 433
Wang X.-F. et al., 2012, ApJ, 749, 126
Wang X.-F., Wang L., Filippenko A. V., Zhang T., Zhao X., 2013, Science, 340, 170
Webbink R. F., 1984, ApJ, 277, 355
Whelan J., Iben I., 1973, ApJ, 186, 1007
Wood-Vasey W. M, Sokoloski J. L., 2006, ApJ, 645, L53
Yoon S.-C., Langer N., 2004, A&A, 419, 623
Yoon S.-C., Langer N., Scheithauer S., 2004, A&A, 425, 217
Yungelson L. R., Livio M., 1998, ApJ, 497, 168
Zuo Z.-Y., Li X.-D., 2014, MNRAS, 442, 1980